Observation of the Ground Subsidence in Gaeun Area Using Permanent Scatterer Interferometric SAR

Hahn-Chul Jung, Sang-Wan Kim, and Joong-Sun Won

Dept. of Earth System Sciences, Yonsei University
134 Shinchon-dong Seodaemun-gu, Seoul, Korea 120-749
hcjung75@hotmail.com

Abstract: This contribution reports on the potential of L-band Permanent Scatterer technique for the detection and monitoring of ground subsidence. We present the use of PS in the abandoned mining area, Korea. Discrete and temporarily stable natural reflectors or permanent scatterers (PS) can be identified from long temporal series of interferometric SAR images. This subset of image pixels can be exploited successfully for high accuracy differential measurements (Ferretti et al., 2000).
Keywords: Permanent Scatterer Technique, Synthetic aperture radar interferometry, Subsidence.

1. Introduction

Causes for ground subsidence at rates higher than a few mm/year include activities as ground water pumping, active and terminated mining, and hydrocarbon extraction. For various reasons there is a demand to monitor such surface deformation. SAR interferometry is one possible technique for surface deformation mapping or one possible element of an integrated monitoring strategy. However, Temporal and geometrical décor-relations often prevent SAR interferometry from being an operational tool for surface deformation monitoring and topographic profile reconstruction. The relative unsatisfying visible spatial resolution in terms of the motion is caused by residual phase noise of the differential interferograms as well. These drawbacks can be overcome by carrying out measurements on a subset of image pixels corresponding to point-wise stable reflectors (or permanent scatterers: PSs) and exploiting a long temporal series of interferometric phases (Colesanti et al., 2003). On these pixels, sub-meter DEM accuracy and millimetric terrain motion detection can be achieved. PSs are identified by means of amplitude dispersion index and coherence of the interferograms. Therefore we can analyze most phenomena that contribute to the phase values such as terrain deformation, DEM errors, orbit indetermination, and atmospheric disturbance.

2. Data and Method

The area of Gaeun is of high geophysical interest because it is known to be very unstable. Since the area is strongly affected by temporal decorrelation, the analysis was carried out in a multi-image framework.

1) Interferogram Formation

We analyzed a series of SAR images between 1992 and 1998 from the Japanese Earth Resources Satellite JERS-1 (L-band, 1.3 GHz, 23.5 cm wavelength) to observe ground surface deformation. The 2-pass was used to derive the differential interferograms indicated in table 1. It illustrates the elapsed time and perpendicular baseline of the used interferometric pairs. The initial baseline estimates based on orbit data were improved rectifying the orbit with a simulated SAR image from DEM.

2) The PS Technique

The permanent Scatterer technique is a further development of the DInSAR method and was invented by Ferretti, Prati, and Rocca at POLIMI, Italy.

Table 1. Summary of JERS-1 interferometric pairs with respect to the master image: 1996/10/27.

No.	Date	Elapsed time [days]	Base perp. [m]
1	1992//11/05	-1452	982.3
2	1992/12/19	-1408	462.2
3	1993/03/17	-1320	554.5
4	1993/06/13	-1232	-635.8
5	1993/07/27	-1188	1002.5
6	1993/09/09	-1144	1285.6
7	1993/10/23	-1100	1034.8
8	1993/12/06	-1056	2117.1
9	1994/01/19	-1012	1464.7
10	1995/02/19	-616	-2399.9
11	1996/03/21	-220	-1309.4
12	1996/07/31	-88	270.1
13	1996/12/10	44	1271.0
14	1997/01/23	88	800.6
15	1997/03/08	132	546.3
16	1997/06/04	220	488.9
17	1997/10/14	352	-3366.1
18	1997/11/27	396	-2210.7
19	1998/01/10	440	-1912.0
20	1998/02/23	484	-2389.2
21	1998/04/08	528	-3181.7
22	1998/05/22	572	571.9
23	1998/07/05	616	-3042.4
24	1998/08/18	660	-1895.3
25	1998/10/01	704	-1557.8

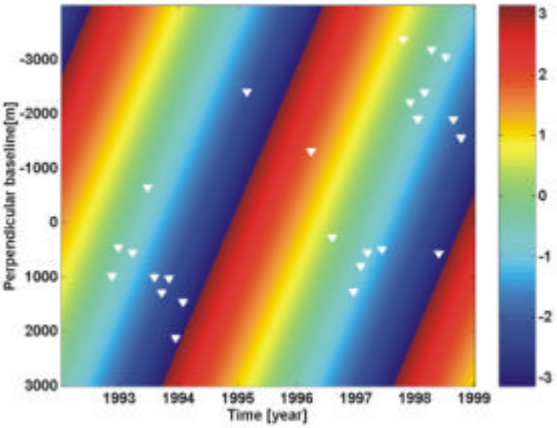

Fig. 1. Space-time distribution of the available data.

In order to identify PS candidates, we calculated the time series of the amplitude values of each pixel in the area of interest as well as coherence map, looking for stable scatterers. After PSC selection, DEM errors and LOS velocities of the PSC were computed by means of an iterative algorithm and then atmospheric components were estimated on the uniform image grid. After atmospheric phase contribution estimation and removal, we could finally compute DEM errors and target velocity on a pixel-by-pixel basis (Ferretti et al., 2001). Fig.1 represents the phase contributions for a LOS velocity of –3 cm/year and a DEM error of 5 m, which were estimated from the 25 wrapped interferograms available.

3. Experimental Results and Discussions

1) PS Identification

As already mentioned, a joint estimation of both DEM error and target velocity was carried out on a pixel-by-pixel basis. Fig. 2 reports an example of the differential phase values plotted vs. normal baseline of each acquisition for a PS, and an example of a time series of the differential phase values for the estimation of the selected point. Each slope of the fitted straight line is the local DEM error and LOS velocity, respectively. Although the results obtained with this technique were remarkable, the algorithm does not cope with nonlinear target motion: coherent scatterers undergoing a complex motion are not identified as PSs, or, in other cases, the nonlinear term of their motion is considered as part of the atmospheric contribution (Prati et al., 2000).

The phase coherence map of the data is shown in fig. 3. The value ranges from zero to one. As this index gets closer to one, it means that phase residue on the pixel is very low after removal of atmospheric components and compensation for LOS velocity and elevation error. Consequently, areas suffering temporal decorrelation look black, whereas stable targets are easily identified. A relation between the PS and the coherent phase can be observed.

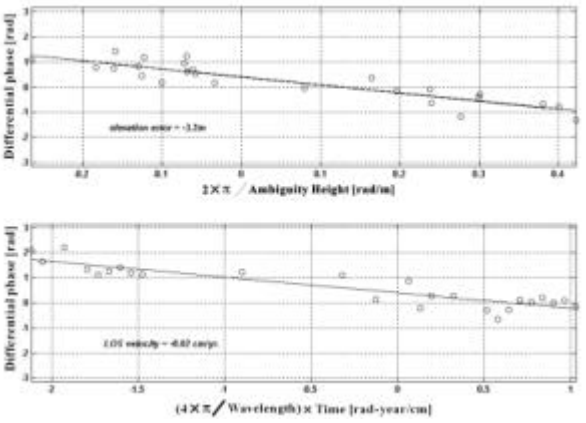

Fig. 2. (a) Differential phase values vs. normal baseline components. (b) Differential phase values vs. time interval components between the slave image and the master image.

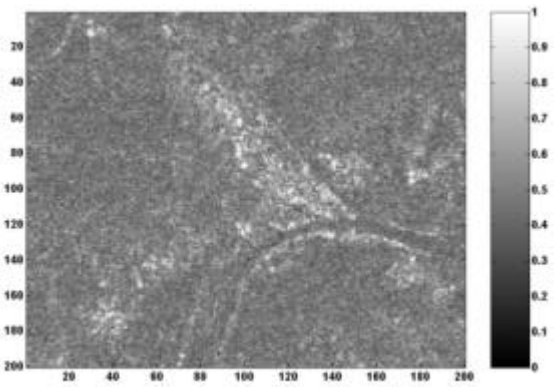

Fig. 3. Phase coherence map after atmospheric phase contribution removal and compensation for LOS velocity and elevation error.

2) DEM Error and LOS Velocity

We see the effect of the DEM refinement carried out by the algorithm with a significant magnification of the vertical dimension in fig. 4. Of course, elevation values can be optimized only where PSs are available.

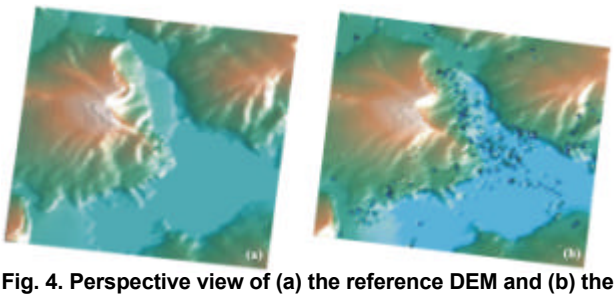

Fig. 4. Perspective view of (a) the reference DEM and (b) the DEM refined in correspondence of the identified PSs For visualization purpose, the vertical axis has been magnified.

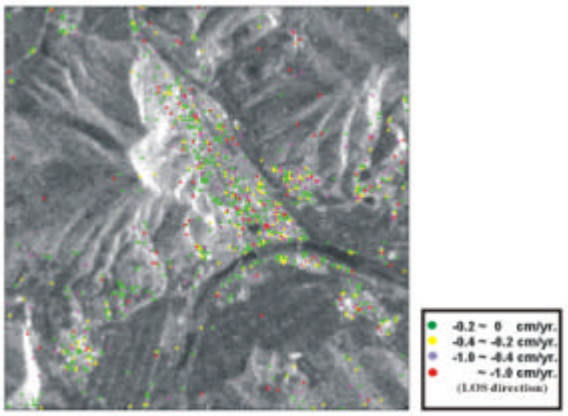

Fig. 5. Estimated LOS velocity and location of a couple of PSs located in the town of Gaeun.

Fig. 5 shows the estimated LOS velocity field on the multi-image reflectivity map obtained using 26 JERS-1 SAR acquisitions. About 1,000 permanent scatterers were identified in the area of investigation. The area is dominantly vegetated. Therefore less longtime stable backscatterers exist and we hardly try to do interpolation with regard to the subsidence of PSs. It could be noted that pixels relative to the vegetated area show low PS density, while higher density can be found in the urbanized area. An average of the cumulated subsidence of PSs was about 3 cm for 6 years. Average LOS deformation rate of every PS depends on the number of available interferograms and on the phase stability of each single PS. As in all differential interferometry applications, results are not absolute both in time and space (Colesanti et al., 2003). Deformation data are referred to the master image (in time) and results are computed with respect to a reference point of known elevation and motion (in space).

4. Conclusions

We measured subsidence occurred in Gaeun area, Korea, from November 1992 to October 1998 using 26 JERS-1 SAR interferograms. Subsidence due to calcite dissolution and abandoned coal mines has been reported in this area. PS usually corresponds to man-made structures such as buildings, dams, penstocks, antenna, pylons as well as stable natural reflectors (e.g. exposed rocks) present on the earth surface. The long time lapse observations made available by this technique allow to estimate long term pixel motion with an accuracy that was previously attainable using optical techniques only (Ferretti et al., 2000).

Further study with comparing with ground measurement data will follow. This study confirms the good potential of L-band PSInSAR to map ground subsidence where is of high temporal decorrelation for vegetated areas.

References

[1] Ferretti, A., Prati, C., Rocca, F., 2000. Nonlinear subsidence rate estimation using Permanent Scatterers in differential SAR interferometry. IEEE Trans. Geosci. Remote Sens. 38(5), 2202-2212.

[2] Ferretti, A., Prati, C., Rocca, F., 2001. Permanent Scatterers in SAR interferometry. IEEE Trans. Geosci. Remote Sens. 39(1), 8-20.

[3] C. Colesanti, A. Ferretti, F. Ferrucci, C. Prati and F. Rocca, "Monitoring known seismic faults using the Permanent Scatterers (PS) Technique", Proceedings of the IGARSS 2000. Vol. 5, pp. 2221-2223.

[4] S.W. Kim, C.W. Lee, J.S. Won, 2002, Ground Subsidence Estimation in a Coastal Reclaimed Land Using JERS-1 L-band SAR Interferometry, Korea Society of Econ. Environ. Geol, 35(5), pp. 465-478.

[5] H. A. Zebker and P. Rosen, 1997, Atmospheric artifacts in interferometric SAR surface deformation and topographic maps, J. Geophys. Res. Solid Earth, vol. 102, no. B4, pp. 7547-7563.

[6] H. A. Zebker and R. Goldstein, 1986, Topographic mapping from SAR observation, J. Geophys. Res., vol. 91, no. B5, pp. 4993-4999.

[7] H. A. Zebker and J. Villasenor, 1992, Decorrelation in interferometric radar echoes, IEEE Trans. Geosci. Remote Sensing, vol. 30, pp. 950-959.

[8] R. Goldstein, 1995, Atmospheric limitations to repeat-pass interferometry, Geophys. Res. Lett., vol. 22, pp. 2517-2520.

[9] D. Massonnet et al., 1993, The displacement field of the landers earthquake mapped by radar interferometry, Nature, vol. 364, pp. 138-142.